Original Research Article

Characterization and Stability Study of Polyurethane / Magnetic Strontium Hexaferrite / Clinoptilolite Nanocomposite

Komeil Azadikhah [a], Mehran Davallo [b, *], Vahid Kiarostami [b], Saeid Mortazavi Nik [c]

[a] PhD Candidate, Department of Chemistry, North Tehran Branch, Islamic Azad University, Tehran, Tehran, Iran
[b] Associate Professor, Department of Chemistry, North Tehran Branch, Islamic Azad University, Tehran, Tehran, Iran
[c] Assistant Professor, Department of Chemistry, North Tehran Branch, Islamic Azad University, Tehran, Tehran, Iran

* Corresponding Author Email: m_davallo@yahoo.com (M. Davallo)   URL: https://www.acerp.ir/article_165206.html

ARTICLE INFO

ABSTRACT

In this research, a new polyurethane / strontium hexaferrite / clinoptilolite (PU/SrM/CLP) nanocomposite was synthesized through the in-situ polymerization method, and its chemical stability in both acidic and alkaline solutions was assessed. It was found that the incorporation of CLP and SrM into the PU matrix would enhance the thermal stability of the nanomaterial. The thermal stability of the composite ingredients against the thermal events up to the temperature of 700 °C in an ascending order includes PU, strontium hexaferrite, and CLP zeolite, respectively. As a result, the formed nanocomposite exhibited more thermal stability than PU. Several analytical techniques such as XRF, XRD, FTIR, SEM-EDX, and BET were employed to characterize the physicochemical properties of the nanocomposite. The presence of FTIR peaks at the wavelengths of 1700 cm^{-1} and 3400 cm^{-1} confirms the C=O and N–H groups due to the formation of PU in the composite structure, respectively. The pore volume and specific surface area of the Nano sorbent using BET were obtained as 0.5978 cm^3/g and 2.60 m^2/g, respectively. Based on the Scherrer equation, the adsorbent crystallite size was measured as 12.76 nm at the highest peak (100 %). In addition, The chemical stability of the prepared nanocomposite was assessed in both acidic and alkaline solutions which showed about a 12 % reduction. The point of zero charge (pH_{pzc}) for nano sorbent was 7.4. According to the obtained results, the PU/SrM/CLP nanocomposite can be utilized as a stable and magnetic sorbent in aqueous harsh media, especially in wastewater samples.

1. INTRODUCTION

A composite material is a combination of various constituents which differ in terms of their physical and chemical properties. When these constituents are combined, they produce a material that is tailored to do a specific job.

Owing to the various properties of the composite materials, they are used in different fields such as wastewater treatment, aerospace, automobile, electronics, construction, energy, biomedical, and other industrial applications [1]. Owing to their excellent physical properties and high adaptability to a chemical structure, polyurethanes (PUs) are extensively applied in

different industrial sectors such as coatings, adhesives, fibers, thermoplastic elastomers, and also the production of porous foams. The PUs are generally formed from the reaction of an isocyanate component with polyol [2]. The fragmented PUs are multi-block copolymers-(X-Y)- which are thermodynamically composed of soft (X) and hard (Y) parts, respectively. At high temperatures, the hard part acts as an efficient reinforcement filler, providing the dimensional stability of the PU by creating a bridge connecting the soft part and elastomeric matrix. Due to the thermodynamic differences, the soft and hard parts in hard use conditions (acidic and strong base and hot solutions) are usually separated by forming a cumulative two-phase network [3]. Despite of excellent properties that PUs have, these compounds are characterized by low thermal stability and mechanical strength. To overcome these drawbacks, some fillers such as heat and impact modifiers can be incorporated into the polymer matrix to enhance their properties. To improve the biodegradability properties of the PUs, biocompatible components such as the hydroxyl group of ricin oleic acid and triglycerides with 90 % C18 fatty acid were introduced into the PU chains. Depending on the nature of the diol and isocyanate fractions, a thermoset or thermoplastic PU can be formed. In case a diol (OHR-OH) forms the soft part and a di inosinate (NCOR-NCO) the hard part, a linear thermoplastic PU will be formed. However, if the ratio of polyisocyanate to polyhydroxy segment is relatively high, the formation of a PU thermostat is quite likely [4]. The structure and properties of the PUs, in addition to the choice of raw materials, depending on the polymerization method, degree of phase separation, hydrogen bonding, morphology, and crystallization rate [5]. PU foam is a new type of organic polymeric material with interesting properties such as low thermal conductivity, chemical inertness, high energy adsorption capacity, and good mechanical strength. There are several reports about the addition of filler particles such as silica to PU, which in turn affects the mechanical and physical properties of these polymers.

In addition, the presence of Magnetic Nanoparticles (MNPs) facilitated control of foam structures, increased mechanical and thermal properties, and improved insulation properties due to its high mechanical, thermal, and magnetic properties in PU foams. Nowadays, the synthesis of new magnetic materials and their composition in polymer matrices has drawn many researchers' attention due to their widespread applications in various fields such as carriers to stabilize microorganisms in water and absorb electromagnetic waves. Despite these advantages, magnetic compounds have at least two major limitations: the limited number of functional groups on the surface and their low dispersion in the polymer matrix. To overcome these limitations and prevent the accumulation of particles in the polymer matrix and increase the interaction chance between the components at the interface, it is suggested that functionalized silages be used for surface modification of the magnetic nanoparticles [6]. Of note, the use of magnetic adsorbents due to their easier separation from the solution with minerals rich in active adsorption sites such as natural zeolite especially Clinoptilolite (CLP) in a polymeric substrate is one of the effective and low-cost methods in dye wastewater treatment [7,8]. The CLP was used in some fields to solve several problems [9-13]. In addition, the application of these mineral particles in harsh conditions such as hot solutions as well as acidic and alkaline environments can change the properties of these minerals and greatly reduce their adsorption properties [14].

In our previous works, several adsorbents including polypyrrole/$SrFe_{12}O_{19}$/graphene oxide [15,16] carbon nanotubes [17], and copper oxide nanoparticles immobilized on activated carbon [18] were fabricated and their characteristics were investigated. In addition, the fabrication of a new composite of ternary components including PU, CLP, and Strontium hexaferrite (SrM) was synthesized in our research group and then employed to adsorb malachite green dye from aqueous solutions and wastewater [19].

This research is the continuation of the previous project that aims to fully characterize the PU/SrM/CLP nanocomposite. The first objective of this project was to determine the chemical stability of the composite material in harsh media using high and low pH_s. Moreover, it assessed the thermal stability of the nanocomposite and compared it with other composite materials.

2. EXPERIMENTAL PROCEDURE

2.1. Materials and Instruments

The Semnan natural zeolite (CLP) powder (Afrand Touska Company, Isfahan, Iran) used in this work with granulation of less than 100×10^{-6} m was provided by the Ministry of Industries and Mines of the Mineralogy Department (Tehran, Iran) as a gift. In addition, $Sr(NO_3)_2.9H_2O$, $Fe(NO_3)_3.9H_2O$, ammonia, citric acid, and other reagents and chemicals with analytical grade were purchased from Merck and Sigma companies. The cationic surfactant of hexadecyl trimethyl ammonium bromide (HDTMA–Br, Merck) with a laboratory grade and purity of 99.99 % (Merck) was provided by the Research Institute of Paint and Coating Science and Technology (Tehran, Iran). The commercial urethane resin (Rokopol RF551, PCC Rokita, Poland) with a viscosity of 4.52 pa.s and average molecular weight of 600 g/mol at 25 °C was also used for the fabrication of rigid PU foams. The 4,4'-Methylene Diphenyl Isocyanate (MDI) hardener with 36 % of NCO groups and a density of 1.57 g/cm^3 at 25 °C was obtained from Yantai Wanhua PUs Group Co (China). Malachite Green Standard (MG)

with a density of 1100×10^3 g/m^3 and a percentage purity greater than 99 % at 20 °C was obtained from Sinopharm chemical reagent company (Shanghai, China).

A Nicolet 8700, Thermo FT-IR spectrometer (USA), A DR-5000–Hach UV-Vis spectrometer (USA), a Scanning Electron Microscopy (SEM, (SIGMA VP-500, ZEISS SEM, Germany)), an RHB2, IKA Centrifuge system (Germany), a Q600 Waters thermogravimetric analyzer (USA), an X-Ray Diffractometer (STADI MP, STOE XRD, Germany) were utilized in this experiment.

2.2. Synthesis and Preparation
2.2.1. Synthesis of Strontium Hexaferrite

The SrM was fabricated through the self-ignition process [20]. First, a mixture of strontium and ferric nitrates with a weight ratio of 2:3 was dissolved in deionized water at 60 °C. The complex of strontium and iron ions was prepared using citric acid and metal ions solution. The solution pH was adjusted at 7 by adding 1:1 water-ammonia solution and stirring it at 80 °C to form a viscous brown gel. Then, the prepared brown gel was placed in a furnace and allowed to reach its combustion temperature. The resulting gel caught fire spontaneously to obtain a compound with a tree-like shape. Subsequently, the collected ash sample was pulverized using an agate mortar and calcined at 450 °C for 1.5 h in the muffle furnace (Nabertherm, LT3/11). Finally, the resulting powder was annealed at 900 °C for 1.5 h to produce SrM.

2.2.2. Preparation of Modified Clinoptilolite

Modification of CLP with HDTMABr was carried out, as reported by Jin and coworkers [21]. Briefly, CLP (60 g) was added into the HDTMABr solution (300 mL, 0.4 % (w/v)), and the solution was shaken at 200 rpm for 23 h at 25 °C on the orbital shaker (GFL3005). Then, centrifugation was performed, and the washing steps were carried out on the final material several times with deionized water. Next, the HDTMABr-modified CLP was placed in an air oven (Binder ED53) at 100 °C for 12 h. The dried material was then pulverized in a vibratory ball mill and was screened through a US 120 mesh screen. The final powder was used for the composite fabrication.

2.2.3. Preparation of Composite

The PU/SrM/CLP nanocomposite was prepared by in-situ polymerization of urethan resin [22] in the presence of SrM and CLP particles using Methylene Diphenyl diisocyanate (MDI), as reported in our previous work [19].

2.3. Characterization

X-Ray Fluorescence (XRF) was utilized to determine the elemental composition of the CLP powders before and followed by surface modification. SEM was employed to study the morphology of the samples. Energy Dispersive X-ray Spectroscopy (EDS) was then used to determine the molar percentage of the elements in the strontium hexaferrite compound. Infrared spectrometers (FT-IR) were subsequently utilized to determine the type of functional groups as well as new bonds formed in the samples. Further, Thermal Gravimetric Analysis (TGA) was used to investigate the thermal behavior of the samples, and X-Ray Diffraction (XRD) analysis to identify the crystal properties of the synthesized nanocomposite. Brunauer-Emmett-Teller (BET) and Langmuir models were developed to study the surface area of the nanocomposite. Brunauer-Joyner-Halenda (BJH) and t–Plot techniques were employed to estimate the pore size distribution, microporous volume, and specific surface area of the nanocomposite, respectively.

2.4. Adsorbent Stability
2.4.1. Thermal Stability

TGA analysis is a method for studying how a substance behaves as a function of temperature. In this work, 5.31 mg of each sample was used and their thermal behavior was evaluated in the temperature range of 25-1350 °C at a rate of 20 °C/min [23,24].

2.4.2. Chemical Stability

The chemical stability of the PU/SrM/CLP composite was studied at both low and high pH values using HCl and NaOH (1 M). First, 0.1 g of the composite was added to 50 ml of NaOH or HCl solution and stored for one week. Then, each sample was filtered and rinsed with double distilled water to achieve a neutral pH. The adsorbent was then dried in an air oven, and its weight losses were recorded during this period. Finally, the adsorption efficiencies of the malachite green dye for the nanocomposite were compared in solutions with and without acid and alkaline [25].

2.5. The pH of Point Zero Charge

The pH of the point of zero charge (pH$_{PZC}$) was computed for the nanocomposite to identify the pH impacts. First, several aliquots of 50 mL of 0.01 M NaCl solution were prepared, and their pH values were adjusted in the range of 2-12 by adding 0.1 M HCl or 0.1 M NaOH solutions dropwise. Then, 0.1 g of adsorbent was added to each flask containing 50 ml of NaCl solution, whose solution pH values had been previously adjusted, and shaken for six hours in airtight conditions at 200 rpm at 25 °C. The pH values of the solution were recorded before and after adding the composite during the processing period. In the next step, the secondary pH values were plotted against the initial pH values. Finally, the pH$_{pzc}$ was determined from the intersection of the curve (The straight line of initial pH$_s$) and the line with the slope of 45° (The line of final pH$_s$) [26].

3. RESULTS AND DISCUSSION

3.1. Acid Washing

Acid washing was performed in a 250 mL flask containing the specific amount of the CLP in 60 min.

Then, X-ray fluorescence spectrometry was used for elemental analysis of the CLP before and after acid washing. No significant changes (Paired t-test, $p > 0.05$) were observed in the elemental composition of CLP before and after acid washing [7]. Therefore, surfactant was used to modify the surface of the CLP, as observed in Table 1.

Table 1. Elemental composition in clinoptilolite before and after acid washing

Sample Percentage	SiO_2 %	Al_2O_3 %	Fe_2O_3 %	CaO %	Na_2O %	MgO %	K_2O %	TiO_2 %	MnO %	P_2O_5 %	L.O.I.[1] %
Before Acid Washing	67.191	11.66	1.205	1.999	1.92	1.428	1.524	0.216	0.014	0.022	12.14
After Acid Washing	68.696	11.81	1.337	1.588	1.231	1.343	1.525	0.219	0.014	0.019	12.16

1- Loss of Ignition

3.2. FTIR Spectra

The FT-IR spectra of the SrM at the three-temperature modes including < 450 °C, > 450 °C, and 900 °C are shown in the wavelength range of 500-4000 cm^{-1}. While no peaks of metal-oxygen bonds were formed (Figure 1a) at temperatures below 450 °C, there is no evidence of hexaferrite formation (Figure 1b) at temperatures above 450 °C. The FT-IR spectrum at temperatures above 900 °C has been determined previously in our published paper [19]. Briefly, at the wavelengths of 435 cm^{-1} and 595 cm^{-1} confirmed the presence of Fe-O stretching vibrations in octagonal and quadrilateral cavities, respectively, indicating the formation of the M-type SrM hexaferrite compound [20]. The observed peaks at about 3500 and 1400 cm^{-1} are attributed to the vibrations of the water molecules present in samples [27].
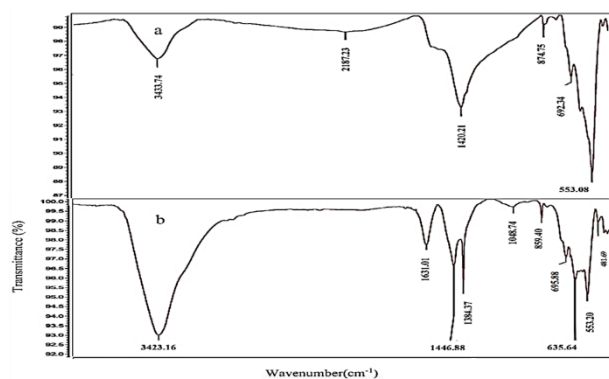

Figure 1. FT-IR spectra of the strontium Hexaferrite at temperatures a) below 450 °C AND b) above 450 °C

The FT-IR spectra of the CLP particles in three states including before acid washing, after acid washing, and after surface modification with HDTMA-Br surfactant are shown in Figure 2. As shown in Figure 2a, the main zeolitic vibrations are located in the ranges of 1069-1077 cm^{-1} (related to Si–O–Si asymmetric stretching vibration) which can be covered by the stretching vibration of (Al–O–Si) and (Al–O), 603–794 cm^{-1} and 496–600 cm^{-1} (related to the stretching vibrations of tetrahedra). The located peak at about 1069 cm^{-1} is present in all zeolitic

structures and sensitive to the framework Si/Al ratio. The located band at about 3400 cm^{-1} for CLP corresponds to the bridging OH groups in Al–OH–Si [28]. Followed by acid washing, the presence of peaks of acidic groups is not significantly different from those of pre-acid washing (Figure 2b). However, after the surface modification of the CLP with a surfactant, the presence of the peaks around 1236 cm^{-1} and 1373 cm^{-1} represents the C-N groups and symmetric bending vibrations of CH3 group of HDTMA-Br surfactant, respectively. The intensive peak at 1752 cm^{-1} is indicative of the stretching vibrational bond of C=O between the surfactant and CLP (Figure 2c) [7].
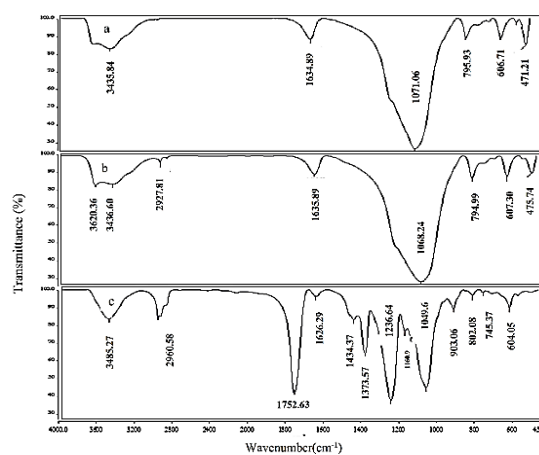

Figure 2. FTIR spectra of clinoptilolite particles in three different states: a) before acid washing, b) after acid washing, and c) after surface modification

3.3. X-Ray Diffraction

The XRD patterns of PU/CLP/SrM composite, SrM, and Modified CLP have been investigated in our published work [19]. Briefly, the presence of PU and hexaferrite reduced the intensity of the XRD peaks of CLP in the nanocomposite. The hexagonal structure of SrM pretreated at a temperature above 900 °C was identified using three characteristic indices (No. 01-080-1198). The characteristic reflection peaks at

about 2θ values of 9.88°, 11.18°, 12.96°, 16.96°,19.50°, 22.36°, 25.19°, 26.04°, and 30.15° are in good agreement with the CLP crystalline structure data file [JCPDS No. 39–1383] [29]. The peaks at about 2θ = 24 and 32 degrees prove the presence of CLP. As observed, the crystallite size depends on different factors such as intensity, peak broadening, sharpness, dislocation density, and strain, which can be calculated through Equation (1) [30].

$$\text{Crystallite Size } (D) = \frac{\kappa\lambda}{\beta\cos\theta} \tag{1}$$

where D is the crystallite size in nm, K is the shape factor which is equal to 0.94, λ the wavelength of X-ray radiation Cu $k_{\alpha 1}$ (λ = 1.5406 Å), β the Full-Width Half Maximum (FWHM) intensity, and θ the Bragg's angle. The dislocation density (δ), lattice constants (a and c), interplanar spacing (d), and unit cell volume (V) were calculated by Equations (2-4). The calculated values are listed in Table 2.

Based on Equation (1) as well as the indices, we have:

$$\text{Dislocation density } (\delta) = \frac{1}{D^2} \tag{2}$$

$$\text{Inter} - \text{planner spacing } \frac{1}{d^2} = \frac{4(h^2 + hk + k^2)}{3a^2} + \frac{l^2}{c^2} \tag{3}$$

$$\text{Volume } (V) = a^2 c \tag{4}$$

3.4. SEM Studies

The SEM images of strontium hexaferrite is shown in Figure 3. The SEM image of the pretreated SrM below 450 °C indicates an almost uniform distribution of the SrM particles (Figure 3a). Upon increasing the temperature up to above 450 °C, the size of the particles will decrease with a relatively more uniform dispersion of nanoparticles (Figure 3b). The SEM images of PU/SrM/CLP nanocomposite has been shown in our published paper [19]. Briefly, increasing the temperature up to above 900 °C, the morphology of nanoparticles generally changed to more irregular shapes, and the size of the SrM nanoparticles reduced to below 100 nanometers. The SrM nanoparticles were aggregated because of the magnetic interaction [31].

3.5. The Surface Characterization

The surface characteristics were compared with those of other methods such as Langmuir, T-Plot, and BJH isotherms, each having specific parameters. The surface characteristics of the synthesized nano sorbent per gram unit such as pore volume and specific surface area according to the Langmuir method were 1.198 $(\text{cm}^3\text{g}^{-1})$ and 5.21 $(\text{m}^2\text{g}^{-1})$, respectively, which is more satisfactory compared to other methods and adsorbents (Figure 4, Table 3) [32].

Table 2. The obtained crystallographic parameters for strontium hexaferrite crystals

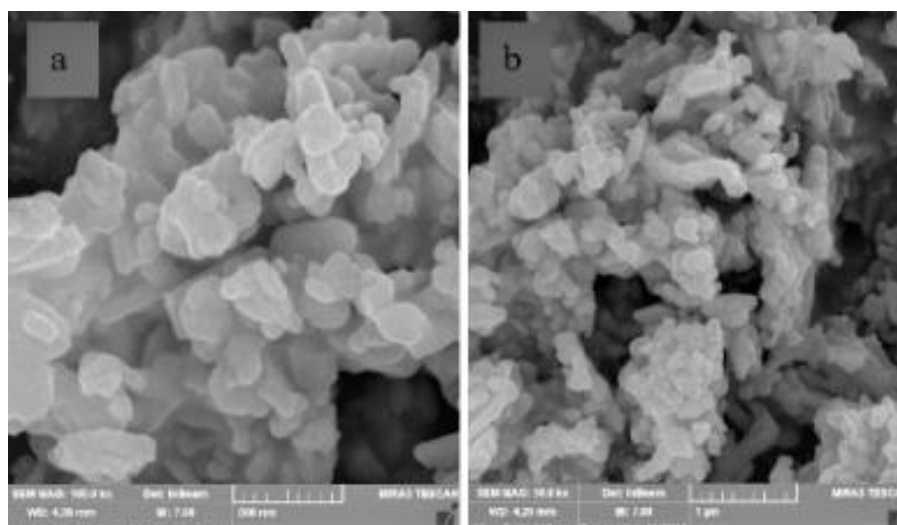| Rel. Int.	2θ	(hkl)	FWHM Left [2θ]	d – Spacing	Crystallite Size	Dislocation Density	Unit Cell Volume
(%)	(degree)	-	β (degree)	$[\text{A}^\theta]$	D $(\times 10^{-9}\text{m})$	$\delta \times 10^{-3}$	$[\text{A}^\theta]^3$
42.57	28.1719	203	0.2666	2.412	5.583	31.169	
65.90	30.4004	110	0.2362	2.94	6.515	42.44	2.49
76.67	32.4399	107	0.1476	2.75	10.212	104.284	
100	34.1528	114	0.1181	2.62	12.76	162.817	

Figure 3. The SEM images of SrM nanoparticles for two conditions including a) below 450 °C and b) above 450 °C
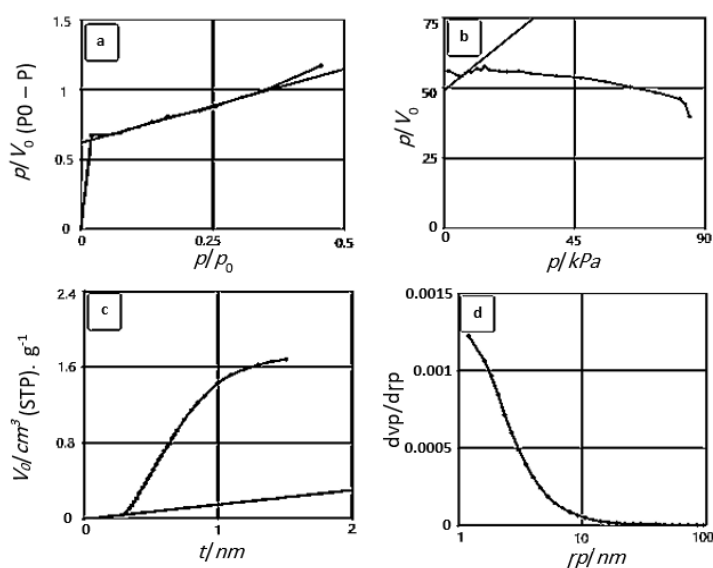
Figure 4. The plots of surface characterization methods include a) BET, b) Longmuir, c) T-Plot, and d) BJH

Table 3. Comparison of the surface parameters of the fabricated nanocomposite with other adsorbents

Samples	Measurement Methods	Surface Features					Ref.
		Pore Volume (cm³g⁻¹)	Special Surface Area (m²g⁻¹)	BET Constant (C)	The Average Diameter of the Cavities (×10⁻⁹ m)	Hole Radius (×10⁻⁹ m)	
PU/SrM/CLP	Langmuir	1.198	5.21	-	-	-	This work
	T -Plot	-	0.237	-	-	-	
	BET	0.5978	2.60	2.69	4.908	-	
	BJH	0.0039	2.93	-	-	1.21	
Pristine Zeolite	Langmuir	1.12	4.9	-	-	-	[23]
CLP Treated by HCl		0.061	20.24	-	-	-	[24]
SBA-15-oz		1.16	711	-	-	-	[25]
ms-OTMS-oz		0.73	945	-	-	-	

3.6. Estimation of Adsorption Mechanism Based on Isothermal Model

The mechanism of the synthesized nanoparticle adsorption is consistent with isotherm type III, in which the graph is convex relative to the P/P0 axis (Figure 5).
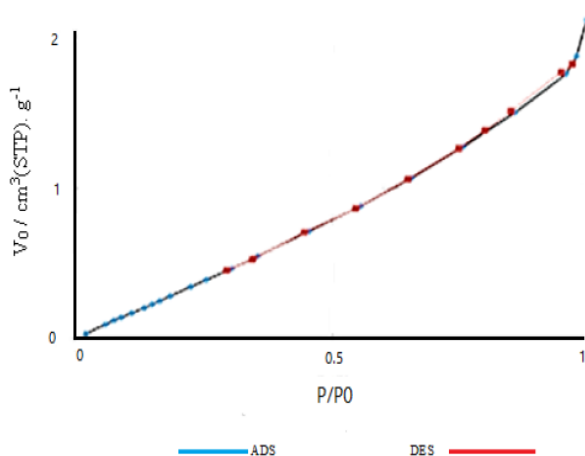

Figure 5. Isothermal Adsorption Diagram of Synthesized Nanocomposite

In this type of adsorption, interactions will occur between the adsorbent molecules in which the adsorption heat is less than the adsorbent heat, indicating that the adsorption process is more interactive between the adsorbent and adsorbed layer than the interaction with the adsorbent surfaces.

This diagram is related to the period when low adsorption occurred on non-porous powders or powders with a diameter greater than the micro size. The swelling point near the end of the adsorption is indicative of the occurrence of adsorption in one layer [32].

3.7. Composite Stability Evaluation
3.7.1. Thermal Stability

The weight loss diagram of the synthesized nanocomposite along with its components versus temperature during the thermal gravimetric method is shown in Figure 6.

The synthesized nanocomposite undergoes a slight weight loss (2 %) during the thermal phenomenon of about 260 °C, which can be attributed to the decomposition of the hard parts of the PU base matrix
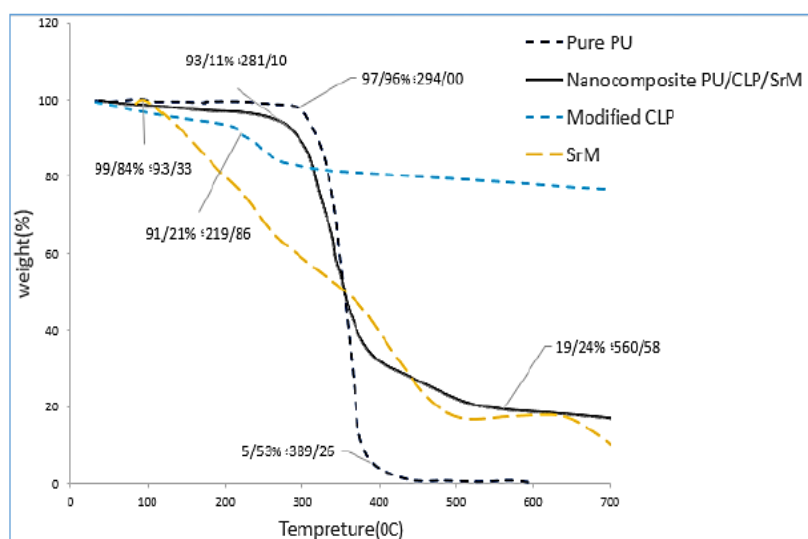
Figure 6. TGA Thermograms of pure PU, Modified CLP, SrM, and PU/SrM/CLP nanocomposite

The greatest weight loss of this nano sorbent (65 %) at the temperature of about 337 °C is due to the removal of the soft parts of the base matrix. This weight loss, however, is less than that of pure PU losing most of its weight (approximately 98 %) at the temperature of 360 °C.

The presence of fillers such as strontium hexaferrite and CLP in the nano sorbent with PU base matrix revealed better thermal stability with less weight loss of 23 % and 18 % at 440 °C and 220 °C, respectively.

The results of the thermal stability of the prepared nanocomposite compared with other adsorbents are shown in Table 4 [31].

Table 4. Thermogravimetric analysis of PU/CLP/SrM nano-composite in comparison with other adsorbents

Adsorbent	stages (°C)	T max (°C)	Mass Loss (%)	Ref.
Pure PU	I 202 - 351	294	2.04	[28]
	II 351 - 535	389	94.47	
Modified CLP	I 202 - 225	219.86	8.79	[27]
SrM Particle	I 60 - 100	93.33	0.16	[31]
PU/Polyglycerol/Bentonite	-	392	50	[26]
PUR/PSO	I 225 - 300	285	3	[17]
	II 300 - 420	358	53	
PU/CLP/SrM	I 240 - 345	281.10	6.89	This Work
	II 345 - 500	470	80.76	

3.7.2. Chemical Stability

The stability of the PU/SrM/CLP nanocomposite was examined by its immersion in a concentrated HCl and also NaOH solution (1 M) for one week. The nanocomposite showed a percentage of weight loss, indicating that the nanocomposite was stable enough in harsh environments. Of note, a comparison of the changes in their adsorption efficiency under the standard malachite green dye solution and the composite without harsh environment showed little difference in their performance when exposed to strong acidic and alkaline environments (Table 5) [25].

Table 5. The chemical stability of the PU/SrM/CLP nanocomposite and comparison of the adsorption efficiency of malachite green (MG) dye in harsh environment

Measured Parameter	Exposed to NaOH	Exposed to HCl	Not exposed to Harsh Environment
Weight Loss (%)	10	12	-
Adsorption Efficiency (%)	86	76.67	99.62
Standard Deviation	2.1	1.35	2.87

3.8. The pH of the Point of Zero Charge

The pH_{PZC} for the nanocomposite was determined in the pH range of 2-12. In the presence of adsorbent, the initial pH of 4 was converted to the final pH of 6.2. However, in alkaline media, the initial pH of 12 was converted to the final pH of 10.3 in the presence of an adsorbent (Figure 7), indicating that in an acidic environment, the adsorbent surface had a positive charge, thus electrostatically adsorbing anion samples. Conversely, if the pH value exceeds the pH_{PZC} value, the surface charge will be negative so that the cations can be adsorbed.

As shown in Figure 7, pH_{pzc} is equal to 7.4, obtained from the intersection of the regression line of the final pH values in presence of the nanocomposite and the line with a slope of 45° degrees (The regression line of the initial pH value in absence of the nanocomposite).
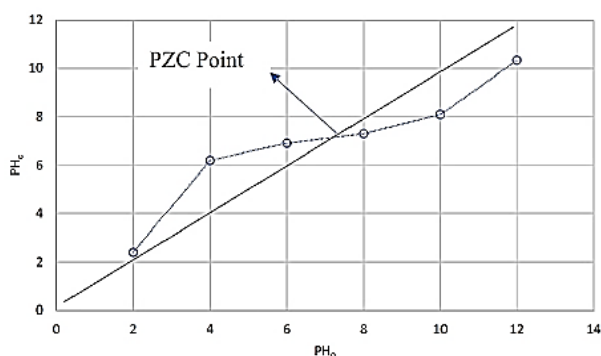
Figure 7. The plot of final pH (pH_f) against the initial pH (pH_0)

To obtain the neutral charge pH point and also find at which point the adsorbent has a neutral charge and tends to change the acidic pH to an alkaline pH, a line between pH 8 and pH 6 with a straight line and slope degree of 45° line was assumed. The line collision with the curve was identified as a point without load or pH_{PZC} equal to 7.4 (Figure 7). At this point, the adsorbent surface charge is zero while at the point above 7.4, the adsorbent tends to remove the positive charge and cationic contaminants. However, at the point below 7.4, the adsorbent tends to remove the negative charge and anionic contaminants [20].

4. CONCLUSION

The thermal analysis showed that the nanocomposite exhibited more thermal stability than polyurethane in the overall temperature range due to its less weight loss percentage. The synthesized nano sorbent mechanism was consistent with isotherm type III, where the diagram was convex relative to the P/P0 axis. This type of adsorption occurred interactively between the adsorbent and the adsorbed layer which was greater than the interaction with the adsorbent surfaces. The point of inflection near the end of the adsorption indicated that the adsorption took place in a single layer. The results obtained from the chemical stability study revealed that the nanocomposite was characterized by suitable thermal stability. In terms of costs, CLP additive as a low-cost natural zeolite is economically viable. Strontium hexaferrite is certainly cost-effective in special applications that require magnetizing the adsorbent and adding proper stability characteristics. Hence, from the results obtained, the PU/SrM/CLP nanocomposite can be utilized as a stable sorbent in aqueous harsh media, especially in wastewater samples.

ACKNOWLEDGMENTS

REFERENCES

1. Chung, D. D. L., *Composite Materials: Science and Applications*, 2nd ed., Springer Science & Business Media, London, (2010). https://doi.org/10.1007/978-1-84882-831-5
2. Alaa, M. A., Yusoh, K., Hasany, S. F., "Pure polyurethane and castor oil based polyurethane: synthesis and characterization", *Journal of Mechanical Engineering and Sciences*, Vol. 8, (2015), 1507-1515. http://doi.org/10.15282/jmes.8.2015.25.014
3. Lan, P. N., Corneillie, S., Schacht, E., Davies, M., Shard, A., "Synthesis and characterization of segmented polyurethanes based on amphiphilic polyether diols", *Biomaterials*, Vol. 17, No. 23, (1996), 2273-2280. https://doi.org/10.1016/0142-9612(96)00056-7
4. Emrani, J., Benrashid, R., Mohtarami, S., Fini, E. H., Abu-Lebdeh, T., "Synthesis and characterization of bio-based polyurethane polymers", *American Journal of Engineering and Applied Sciences*, Vol. 11, No. 4, (2018), 1298-1309. https://doi.org/10.3844/ajeassp.2018.1298.1309
5. Jiang, L., Ren, Z., Zhao, W., Liu, W., Liu, H., Zhu, C., "Synthesis and structure/properties characterizations of four polyurethane model hard segments", *Royal Society Open Science*, Vol. 5, No. 7, (2018), 180536. https://doi.org/10.1098/rsos.180536
6. Nikje, M. M. A., Akbar, R., Ghavidel, R., Vakili, M., "Preparation and characterization of magnetic rigid polyurethane foam reinforced with dipodal silane iron oxide nanoparticles Fe₃O₄@APTS/GPTS", *Cellular Polymer*, Vol. 34, No. 3, (2015), 137-156. https://doi.org/10.1177/026248931503400302
7. Ebrahimi, R., Maleki, A., Shahmoradi, B., Rezaee, R., Daraei, H., Safari, M., Zandsalimi, Y., Bahmani, P., Harkaranahalli Puttaiah, S., "Organic dye removal from aqueous media by using acid modified Clinoptilolite", *Journal of Advances in Environmental Health Research*, Vol. 6, No. 2, (2018), 118-127. https://doi.org/10.22102/jaehr.2018.132980.1080
8. Armağan, B., Özdemir, O., Turan, M., Celik, M. S., "The removal of reactive azo dyes by natural and modified zeolites", *Journal of Chemical Technology & Biotechnology: International Research in Process, Environmental & Clean Technology*, Vol. 78, No. 7, (2003), 725-732. https://doi.org/10.1002/jctb.844
9. Pourtaheri, A., Nezamzadeh-Ejhieh, A., "Enhancement in photocatalytic activity of NiO by supporting onto an Iranian clinoptilolite nano-particles of aqueous solution of cefuroxime pharmaceutical capsule", *Spectrochimica Acta Part A: Molecular and Biomolecular Spectroscopy*, Vol. 137, (2015), 338-344. https://doi.org/10.1016/j.saa.2014.08.058
10. Nezamzadeh-Ejhieh, A., Tavakoli-Ghinani, S., "Effect of a nano-sized natural clinoptilolite modified by the hexadecyltrimethyl ammonium surfactant on cephalexin drug delivery", *Comptes Rendus Chimie*, Vol. 17, No. 1, (2014), 49-61. https://doi.org/10.1016/j.crci.2013.07.009
11. Sharifian, S., Nezamzadeh-Ejhieh, A., "Modification of carbon paste electrode with Fe (III)-clinoptilolite nano-particles for simultaneous voltammetric determination of acetaminophen and ascorbic acid", *Materials Science and Engineering: C*, Vol. 58, (2016), 510-520. https://doi.org/10.1016/j.msec.2015.08.071
12. Nezamzadeh-Ejhieh, A., Afshari, E., "Modification of a PVC-membrane electrode by surfactant modified clinoptilolite zeolite towards potentiometric determination of sulfide", *Microporous and Mesoporous Materials*, Vol. 153, (2012), 267-274. https://doi.org/10.1016/j.micromeso.2011.12.054
13. Tamiji, T., Nezamzadeh-Ejhieh, A., "Sensitive voltammetric determination of bromate by using ion-exchange property of a Sn (II)-clinoptilolite-modified carbon paste electrode", *Journal of Solid State Electrochemistry*, Vol. 23, No. 1, (2019), 143-157. https://doi.org/10.1007/s10008-018-4119-4

14. Heard, C. J., Grajciar, L., Uhlík, F., Shamzhy, M., Opanasenko, M., Čejka, J., Nachtigall, P., "Zeolite (in) stability under aqueous or steaming conditions", *Advanced Materials*, Vol. 32, No. 44, (2020), 2003264. https://doi.org/10.1002/adma.202003264

15. Ebrahimpoor, S., Kiarostami, V., Khosravi, M., Davallo, M., Ghaedi, A., "Bees metaheuristic algorithm with the aid of artificial neural networks for optimization of acid red 27 dye adsorption onto novel polypyrrole/SrFe$_{12}$O$_{19}$/graphene oxide nanocomposite", *Polymer Bulletin*, Vol. 76, (2019), 6529-6553. https://doi.org/10.1007/s00289-019-02700-7

16. Ebrahimpoor, S., Kiarostami, V., Khosravi, M., Davallo, M., Ghaedi, A., "Optimization of tartrazine adsorption onto polypyrrole/SrFe$_{12}$O$_{19}$/graphene oxide nanocomposite using central composite design and bat-inspired algorithm with the aid of artificial neural networks", *Fibers and Polymers*, Vol. 22, (2021), 159-170. https://doi.org/10.1007/s12221-021-8163-9

17. Vafaei, A., Ghaedi, A. M., Avazzadeh, Z., Kiarostami, V., Agarwal, S., Gupta, V. K., "Removal of hydrochlorothiazide from molecular liquids using carbon nanotubes: Radial basis function neural network modeling and culture algorithm optimization", *Journal of Molecular Liquids*, Vol. 324, (2021), 114766. https://doi.org/10.1016/j.molliq.2020.114766

18. Ghaedi, A. M., Karamipour, S., Vafaei, A., Baneshi, M. M., Kiarostami, V., "Optimization and modeling of simultaneous ultrasound-assisted adsorption of ternary dyes using copper oxide nanoparticles immobilized on activated carbon using response surface methodology and artificial neural network", *Ultrasonics Sonochemistry*, Vol. 5, (2019), 264-280. https://doi.org/10.1016/j.ultsonch.2018.10.007

19. Azadikhah, K., Davallo, M., Kiarostami, V., Mortazavinik, S., "Modeling of malachite green adsorption onto novel polyurethane/SrFe$_{12}$O$_{19}$/clinoptilolite nanocomposite using response surface methodology and biogeography-based optimization-assisted multilayer neural network", *Environmental Science and Pollution Research*, Vol. 29, No. 24, (2022), 36040-36056. https://doi.org/10.1007/s11356-021-18249-w

20. Masoudpanah, S. M., Ebrahimi, S. S., "Synthesis and characterization of nanostructured strontium hexaferrite thin films by the sol–gel method", *Journal of Magnetism and Magnetic Materials*, Vol. 324, No. 14, (2012), 2239-2244. https://doi.org/10.1016/j.jmmm.2012.02.109

21. Jin, X., Yu, B., Chen, Z., Arocena, J. M., Thring, R. W., "Adsorption of Orange II dye in aqueous solution onto surfactant-coated zeolite: Characterization, kinetic and thermodynamic studies", *Journal of Colloid and Interface Science*, Vol. 435, (2014), 15-20. https://doi.org/10.1016/j.jcis.2014.08.011

22. Peng, H. K., Wang, X. X., Li, T. T., Huang, S. Y., Lin, Q., Shiu, B. C., Lou, C. W., Lin, J. H., "Effects of hydrotalcite on rigid polyurethane foam composites containing a fire retarding agent: compressive stress, combustion resistance, sound adsorption, and electromagnetic shielding effectiveness", *RSC Advances*, Vol. 8, No. 58, (2018), 33542-33550. https://doi.org/10.1039/C8RA06361C

23. Filip, D., Macocinschi, D., "Thermogravimetric analysis of polyurethane – polysulfone blends", *Polymer International*, Vol. 51, No. 8, (2002), 699-706. https://doi.org/10.1002/pi.972

24. Filip, D., Macocinschi, D., Vlad, S., "Thermogravimetric study for polyurethane materials for biomedical applications", *Composites Part B: Engineering*, Vol. 42, No. 6, (2011), 1474-1479. https://doi.org/10.1016/j.compositesb.2011.04.050

25. Talley, K., Alexov, E., "On the pH-optimum of activity and stability of proteins", *Proteins: Structure, Function, and Bioinformatics*, Vol. 78, No. 12, (2010), 2699-2706. https://doi.org/10.1002/prot.22786

26. Fiol, N., Villaescusa, I., "Determination of sorbent point zero charge: usefulness in sorption studies", *Environmental Chemistry Letters*, Vol. 7, (2009), 79-84. https://doi.org/10.1007/s10311-008-0139-0

27. Iazdani, F., Nezamzadeh-Ejhieh, A., "FeO-Clinoptilolite nanoparticles: Brief characterization and its photocatalytic kinetics towards 2,4-dichloroaniline", *Chemical Physics*, Vol. 550, (2021), 111305. https://doi.org/10.1016/j.chemphys.2021.111305

28. Nezamzadeh-Ejhieh, A., Shirzadi, A., "Enhancement of the photocatalytic activity of Ferrous Oxide by doping onto the nano-clinoptilolite particles towards photodegradation of tetracycline", *Chemosphere*, Vol. 107, (2014), 136-144. https://doi.org/10.1016/j.chemosphere.2014.02.015

29. Manikandan, B., Murali, K. R., John, R., "Optical, Morphological and Microstructural Investigation of TiO$_2$ nanoparticles for Photocatalytic application", *Iranian Journal of Catalysis*, Vol. 11, No. 1, (2021), 1-11. https://ijc.shahreza.iau.ir/article_680810.html

30. Samandari, M., Taghva Manesh, A., Hosseini, S. A., Mansouri, S., "Process Optimization and Kinetic study of Wet Peroxide Oxidation of Phenol in Wastewater over Mg-Al Nano Mixed Oxide", *Iranian Journal of Catalysis*, Vol. 11, No. 2, (2021), 175-180. https://ijc.shahreza.iau.ir/article_682697.html

31. Trovati, G., Sanches, E. A., Neto, S. C., Mascarenhas, Y. P., Chierice, G. O., "Characterization of polyurethane resins by FTIR, TGA, and XRD", *Journal of Applied Polymer Science*, Vol. 115, No. 1, (2010), 263-268. https://doi.org/10.1002/app.31096

32. Bardestani, R., Patience, G. S., Kaliaguine, S., "Experimental methods in chemical engineering: specific surface area and pore size distribution measurements-BET, BJH, and DFT", *The Canadian Journal of Chemical Engineering*, Vol. 97, No. 11, (2019), 2781-2791. https://doi.org/10.1002/cjce.23632